SUPPLEMENTAL DATA AND METHODS

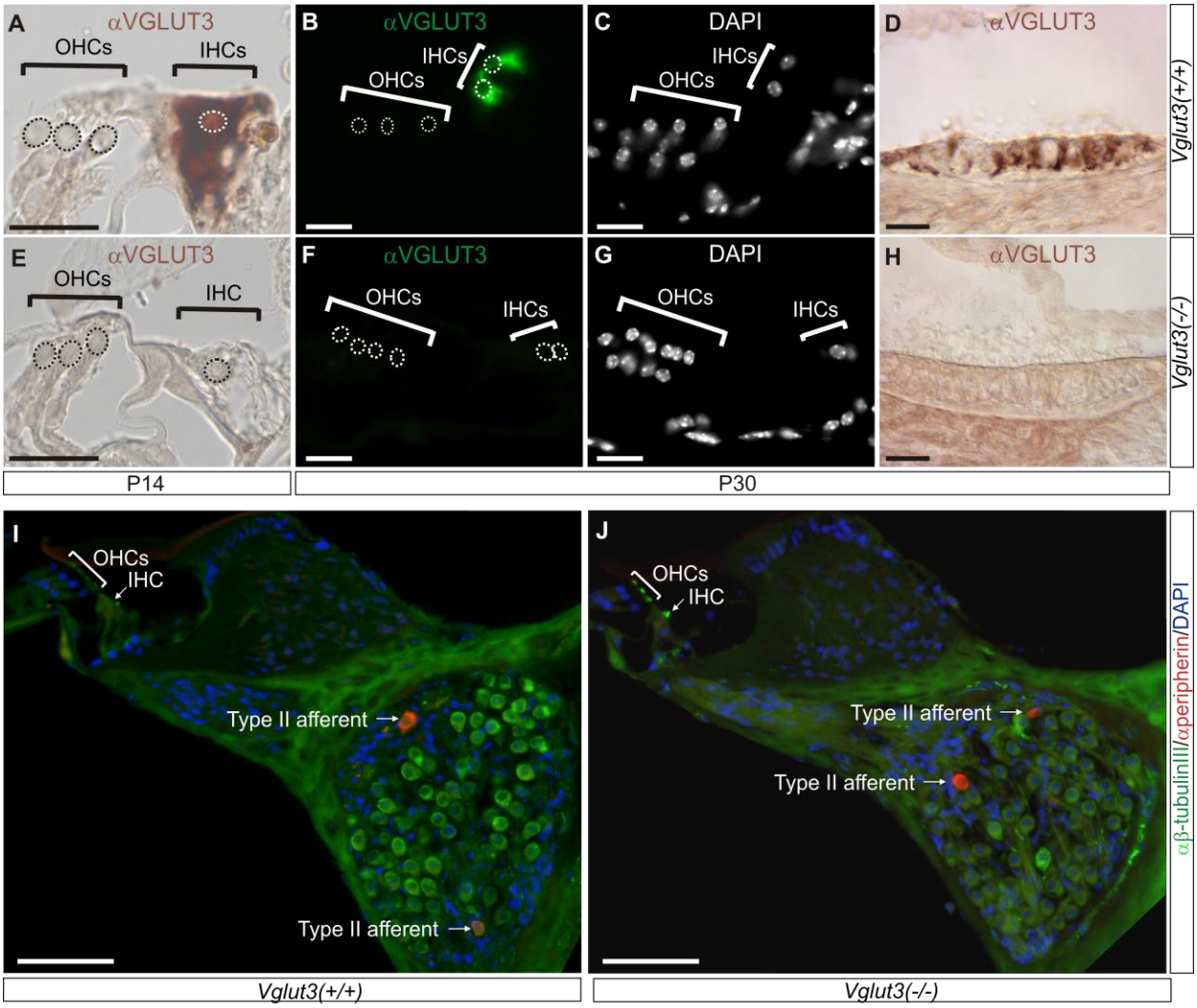

K

Genotype	Total SGN density (cells/mm²)	Type I SGN density (cells/mm²)	Type II SGN density (cells/mm²)
Vglut3(+/+) n = 3	2175 ± 86	2076 ± 87	99.9 ± 23
Vglut3(-/-) n = 3	1762 ± 90	1658 ± 80	104 ± 22
p value	3.95E-07	8.14E-08	0.36

Supplemental Figure S1: VGLUT3 is expressed in cochlear IHCs but not OHCs (related to figure 1). Amplified immunohistochemistry with an antibody to VGLUT3 using ABC/DAB reaction on P14 (**A**,**E**), P30 (**D**,**H**) and tyramide amplification on P30 (**B**,**F**, with the nuclear pattern indicated in **C**,**G**) inner ear reveals that cochlear inner hair cells (IHCs), and hair cells of the saccular macula, but not outer hair cells (OHCs), express VGLUT3 protein. Lack of immunoreactivity in inner ears from *Vglut3*$^{-/-}$ mice (**E**-**H**) confirms that immunoreactivity in wild type specifically detects VGLUT3 proteins. Dashed lines outline nuclei. Scale bars are 20 µm.

(**I**,**J**) Immunohistochemistry on sections of *Vglut3*$^{+/+}$ and *Vglut3*$^{-/-}$ with a marker of spiral ganglion neurons (anti-βIII tubulin) and a marker of type-II afferents (anti-Peripherin) allows a quantification of the loss of type-I and -II afferents in the absence of VGLUT3. (**K**) Neuronal counts (average ± SD) show that the reported decline [S1] in spiral ganglion neurons (SGN) in *Vglut3*$^{-/-}$ mice is due to loss of type-I but not type-II afferents, consistent with functional expression of VGLUT3 in inner but not outer hair cells. P values are based on Student's *t*-test. Sample size n=3 mice per genotype.

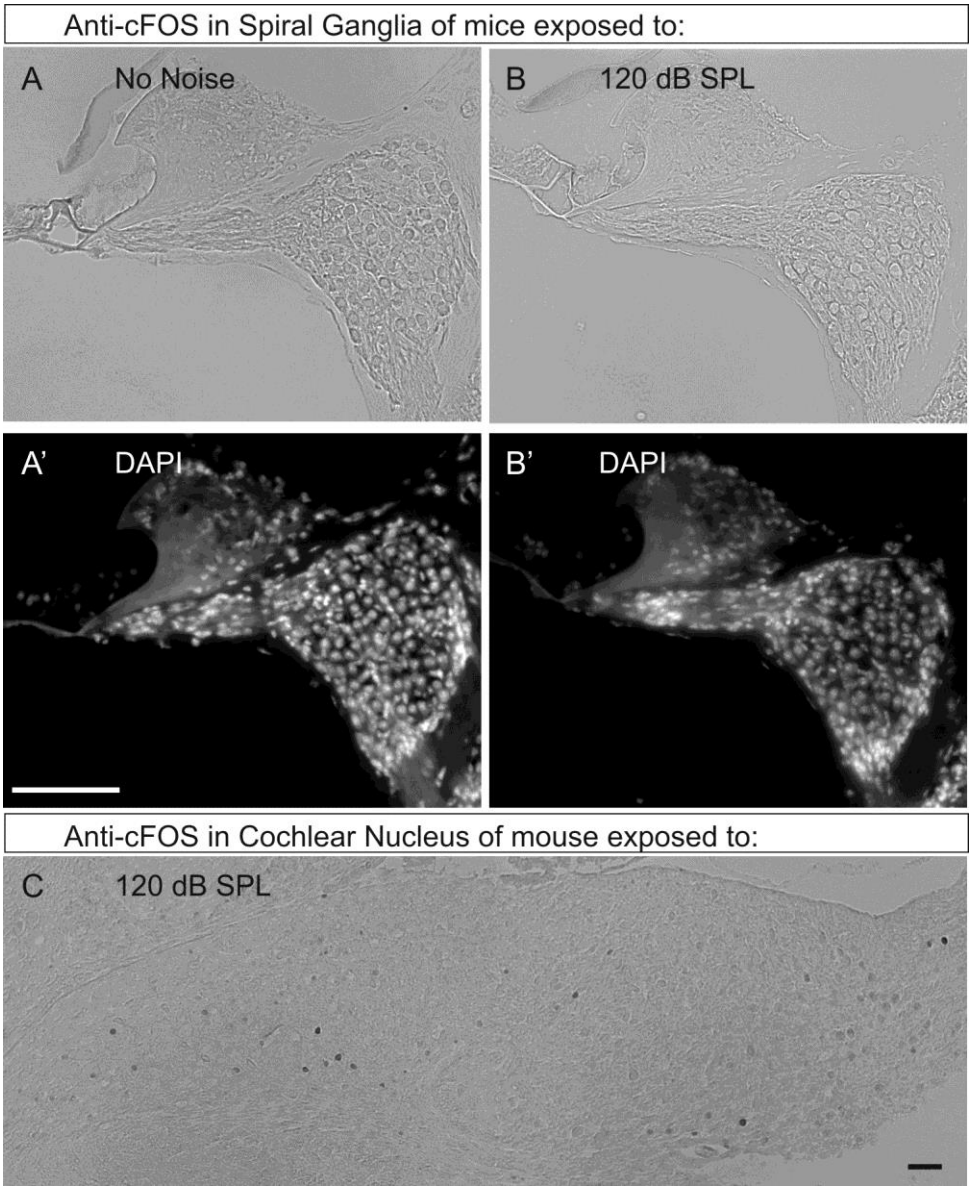

Supplemental Figure S2 (related to figure 2). Noise exposure induces cFOS upregulation in neurons of cochlear nucleus, but not of the spiral ganglion. Immunohistochemistry with antibodies to cFOS in sections of (A,B) cochlea and (C) cochlear nucleus of wild type mice exposed to (A) no noise and (B,C) 120 dB SPL octave-band noise (8-16 kHz) for 1 hr. Cochlea in (B) and cochlear nucleus in (C) are from the same animal and were processed in parallel with the same experimental conditions, including decalcification. (A',C') DAPI labeling of the nuclei corresponding to sections in (A,B). In our experiments, noise exposure induced cFOS in cochlear nucleus (see more examples in figures 2 and 3), but not in neurons of the cochlear spiral ganglion. Scale bars are 50 μm.

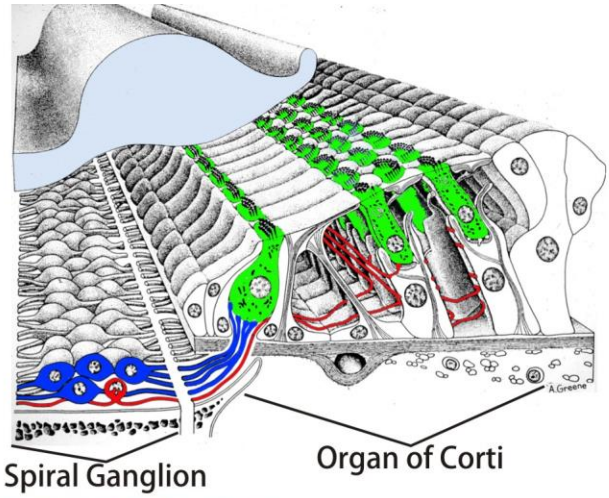

Type II afferents
Type I Afferents
Hair Cells

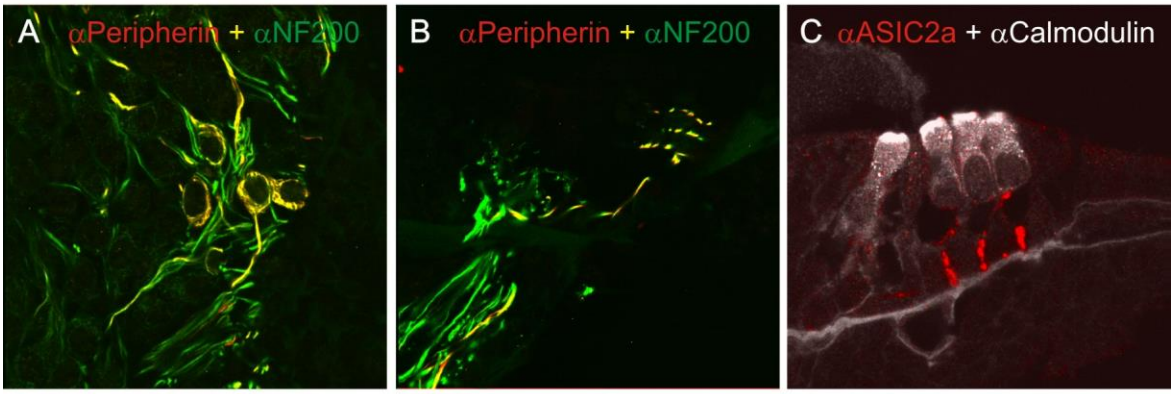

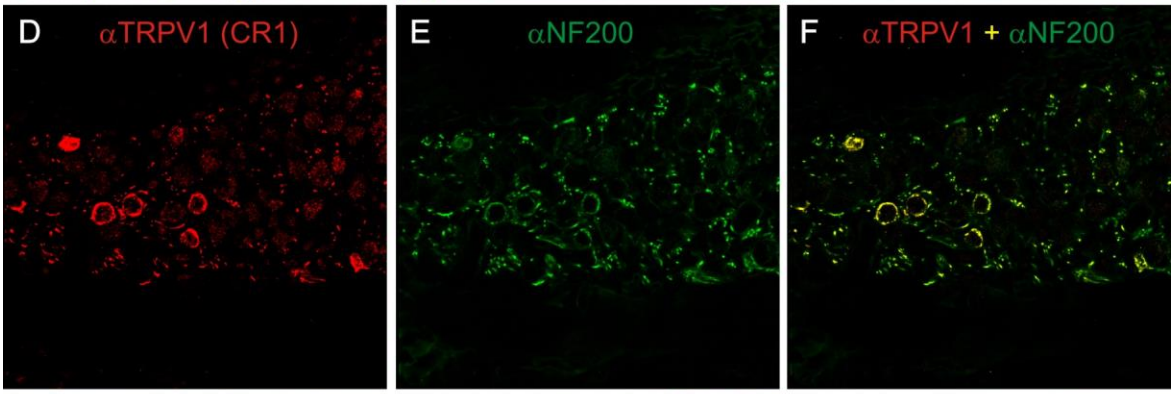

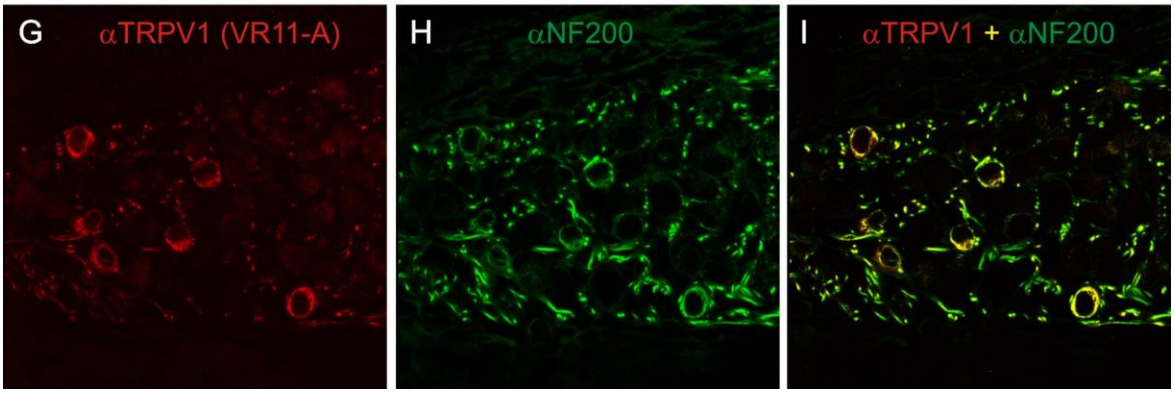

Supplemental Figure S3: Antibodies to nociceptive proteins or markers label cochlear type-II afferents (related to figure 3). (Top) Schematic representation of the cochlea, with type-I afferent (blue) and type-II afferent (red) neuronal bodies in the spiral ganglion and their processes under the hair cells (red) in the organ of Corti (modified from [S2]). (A, B) Antibodies to Neurofilament 200 (mouse monoclonal clone RT97, Biodesign International) label (in green) the processes of both type-I and -II afferents (B) and, at 1/100 dilution, also label the somas of type-IIs preferentially [S3] (A,E,H). Antibodies to peripherin (Rabbit AB1530, Chemicon International), which in somatosensory ganglia label small-diameter nociceptors, label (in red) cochlear type-II afferents, as previously reported [S4]. (C) Antisera (R6798; [S5]) to Acid Sensing Ion Channel 2a (ASIC2a, formerly known as BNaC1α;) labels the terminal processes of type-II afferents (red) extending under the three rows of outer hair cells. Antisera to calmodulin (mouse monoclonal clones 2D1+1F11+6D4; Product # C7055, Sigma) label (white) postnatal hair cell. The much more numerous type-I afferents, which terminate in the inner hair cells, are not labelled with anti-ASIC1a. (D-I) Immunohistochemistry with antibodies raised against the intracellular c-terminal portion of the capsaicin receptor (TRPV1), a major detector of heat, low pH and other nociceptive signals, label the soma of cochlear type-II afferents. Three different antibodies labelled type-IIs: Rabbit anti-Capsaicin Receptor (CR1, stock B390-1, Euro-Diagnostica) (D), rabbit anti-Rat Vanilloid Receptor 1 (VR11-A, Alpha Diagnostic International) (G), and mouse anti-Capsaicin Receptor (MAB5568, Millipore) (not shown). However an antibody to the N-terminus of TRPV1 (VR1 N-terminus, Neuromics) did not label type-IIs, suggesting that if these immunoreactivities represent TRPV1 protein, it may be the splice variant lacking most of the cytosolic N-terminus and whose mRNA has been detected in the cochlear spiral ganglion [S6]. Anti-NF200 (RT97, in green) confirms that the cell bodies are of type-II afferents. The three antibodies to TRPV1 that labelled type-II did not label the terminals of type-II afferents under the OHCs, but they also do not label the peripheral terminals of somatosensory nociceptors despite functional evidence of their presence at such terminals [S7]. Neuronal cell bodies and processes labelled with green and red fluorophores appear yellow. Immunohistochemistry was on frozen sections of postnatal mouse cochlea and images depict either the spiral ganglion (A,D-I) and the organ of Corti (B,C).

E

Sp5	No Noise	80 dB	120 dB
WT	0.12±0.18 (n=2)	1.16±0.92 (n=3)	0.97±0.63 (n=4)
KO	0.90±0.80 (n=3)	1.50±0.94 (n=3)	0.66±0.14 (n=4)

F

VeNu	No Noise	80 dB	120 dB
WT	0.57±0.69 (n=4)	0.26±0.26 (n=3)	0.93±0.63 (n=4)
KO	0.05±0.09 (n=3)	0.53±0.52 (n=3)	0.35±0.21 (n=4)

Supplemental Figure S4: Tissue-damaging noise does not activate neurons in vestibular or trigeminal nuclei (related to figure 4). (**A-D**) Locations of cFos-expressing cells (red dots) in coronal brainstem sections from wild type (A,B) and *Vglut3*$^{-/-}$ (C,D) mice exposed to noxious noise (8-16 kHz at 120 dB SPL for 1 hr; A,C) or to no noise (also for 1 hr; B,D). Noxious noise causes cFos expression in neurons of cochlear (CN) but not vestibular (VeNu) or trigeminal (Sp5) nuclei. (E,F) Average densities (±SD) of cFos+ neurons in trigeminal (E) and vestibular (F) nuclei averaged from several mice exposed to noxious (120 dB), innocuous (80 dB) or no noise (n=number of mice of each genotype and sound exposure level). There is no significant difference in cFos+ densities between nuclei of mice exposed to noxious noise or to innocuous or no noise (Type III F-test; $P>0.05$ for all pairwise comparisons).

Supplemental Experimental Procedures

Animals. All animal care and procedures were carried out according to the Northwestern University Institutional Animal Care and Use Committee in compliance with the National Institutes of Health standards. Mice were housed up to 5 animals per cage in the barrier rooms of Northwestern University's animal facility and maintained on a 12-h light/dark cycle with lights turned on at 7:00am. VGLUT3 null mutant mice in a C57BL/6 background were generated as previously described [S1] and were provided by Robert Edwards, PhD. VGLUT3 heterozygous breeding pairs were mated to produce male and female *Vglut3*$^{-/-}$,*Vglut*$^{+/-}$and *Vglut3*$^{+/+}$ littermates from 10 different litters.

Tissue processing. Unfixed (P14) inner ears were dissected following isoflurane overdose and postfixed for 1 hr in 4% paraformaldehyde. Fixed (P60 and P240) tissues were dissected following cardiac perfusion with 4% paraformaldehyde, postfixed for 1 hour (inner ears) or overnight (brains). All ears were decalcified with RDO (Electron Microscopy Sciences). Tissues were taken through a sucrose gradient of 10%, 20%, 30% sucrose, frozen in OCT and cryosectioned at 12 microns.

Amplified Immunohistochemistry to VGLUT3. P14; P30 wild type and *Vglut3*$^{-/-}$ inner ears from either sex were examined for VGLUT3 expression. Hair cells were labeled with anti-VGLUT3, 1:2500, from Robert Edwards. All tissue sections were postfixed in 2% paraformaldehyde for 10 minutes, and endogenous peroxidase quenched using 1% H_2O_2, 10% Methanol in 1X PBS for 30 min. Tissue was blocked in either 1% TSA block or 10% serum followed by overnight incubation with primary antibody at 4˚C. The following secondary antibodies were used: GP anti-donkey-HRP or GP anti-donkey-biotin (1.100, Jackson Immunoresearch). Signal amplification was performed with Alexa488 tyramide (1:150, TSA; Invitrogen) or ABC/DAB reaction (avidin-biotin complex with diaminobenzidine reaction, Vector Laboratories).

Additional immunohistochemistry was performed on frozen sections of neonatal (P1-10) mouse cochleae as previously detailed [S5, S8]. Antisera used were monoclonal mouse anti-Neurofilament 200 (clone RT97, Biodesign International; 1/100 dilution), monoclonal mouse anti-Calmodulin (clones 2D1+1F11+6D4; Product # C7055, Sigma; 1/100 dilution), rabbit anti-Peripherin (Rabbit AB1530, Millipore; 1/100), Rabbit anti-BNaC1α (aka ASIC2a) (R6798; [S5]), Rabbit anti-Capsaicin Receptor (CR1, stock B390-1, Euro-Diagnostica), rabbit anti-Rat Vanilloid Receptor 1 (VR11-A, Alpha Diagnostic International), and monoclonal mouse anti-Capsaicin Receptor (MAB5568, Millipore). In adult frozen sections of cochlea, hair cells were labelled with rabbit anti-Myosin-VIIa (25-6790, Proteus Bioscience, 1/200).

Image Collection. All images were acquired using a Nikon E600 pan fluorescence microscope equipped with a CCD camera (Spot RC-slider).

Spiral ganglion neuronal densities. P60 wild type and *Vglut3*$^{-/-}$ cochlea from either sex were processed for spiral ganglion cell counts. Mouse monoclonal anti-β-Tubulin III (T8660, Sigma, at 1:500) was used to label all SGN, and rabbit anti-peripherin (AB1530, Millipore, at 1:500) to label type-II SGN. Nuclei were visualized using a DAPI fluorescent counterstain (1:1000, Life Technologies). 20X images of midmodiolar cochlear cross sections were collected. Image J was used to outline the spiral ganglion and generate the area. Quantitative assessment was performed on every other cross section to reduce chances of double counting. Labeled cells were counted only if they had a round cell body, presence of nucleus, and homogenous cytoplasm. Densities were calculated and statistical differences were measure using a student's t test (GraphPad Prism; GraphPad Software Inc.).

Loud Noise Avoidance. We tested for behavioral avoidance to intense noise by male and female (P60) *Vglut3*$^{-/-}$, *Vglut3*$^{+/-}$, and *Vglut3*$^{+/+}$ mice. Animals of each genotype were tested consecutively between the hours of 9am – 5pm in a quiet room, where endogenous noise levels did not register above 60 dB SPL. In this assay, mice are presented a choice between two interconnected compartments: one in which octave-band noise (8-16 kHz) is presented at 100, 105, 115 or 120 dB SPL and another where the sound level is attenuated by ~25 dB. We used a custom built plexiglass chamber (22.5 cm long x 34 cm wide x 10 cm high) with two identical compartments (22.5 cm long x 17 cm wide x 10 cm high) each connected to a speaker (JBL, 2426H). All walls were coated with sound absorbing foam (Soundcoat) to facilitate the dampening of sound from the "noisy" to the "quiet" compartment (see below). Small circular holes (diameter of 3 cm) were constructed on each side of the compartments to provide a passage way for the mouse to move freely. We alternated 2 min-long periods in which noise was applied through a speaker to one of the chambers with 2-min intervals during which no noise was applied. The animal is free to move between the compartments, and hence to avoid the intense noise. In order to eliminate chamber bias or learning effects, we moved the noise from one chamber to the other after each noise exposure. We video recorded for one hour and then measured the time spent in the "noisy" and attenuated compartments. The amount of time animals spent in the noisy and quiet compartments during pre-trials and noise exposure trials was averaged. Statistical differences were measured using an unpaired student's t-test to test the null hypothesis that the means of two populations are equal (GraphPad Prism; GraphPad Software Inc., San Diego, CA, USA).

Noise was generated by a 15 MHz Arbitrary Waveform Generator (HP 33120A), and the output was amplified by a Hafler (P1500) Professional Amplifier and bandpassed at 8-16 KHz by a Stewart VBF8 Filter. Noise levels were measured with a sound level meter (RS 33-2055) in seven distinct locations within the noisy compartment and ranged within 3 dB of the selected intensity. Sound pressure levels were also recorded in seven locations within the adjacent quiet compartment and were found to range between 68-80 dB. Location of the animals during pre-trials and noise trials were recorded using a mounted Canon Mini DV camcorder (Zr 200) and transferred to a computer containing Real Player for blind scoring.

Noxious-Noise neuronal Response:
Noise Exposure. Adult male and female (P60) *Vglut3*$^{+/+}$ and *Vglut3*$^{-/-}$ mice were used for 1 hr exposure to broadband (8-16 kHz) or no noise. 120 db SPL was chosen for noxious noise delivery as it causes loss of OHCs and permanent threshold shifts (PTS) [S9]. 80 db SPL was chosen for innocuous noise delivery as it does not cause loss of OHCs or PTS [S9] . In the *Vglut3*$^{-/-}$ group: 4 mice were exposed to 80 dB, 4 mice to 120 dB, and 5 mice were used as no-noise controls. In the *Vglut3*$^{+/+}$ group: 4 mice were exposed to 80db, 3 mice to 120dB, and 4 mice were used as no-noise controls. Animals of each genotype were exposed consecutively (by ENF) to noise or no noise in a sound proof booth. We built a plexiglass chamber (22.5 cm long x 17 cm wide x 10 cm high) connected to a speaker (JBL, 2426H). The animals were allowed to acclimate to the chamber for one hour. Immediately following, noise was delivered for one hour, or remained off for the no-noise controls. Noise was generated by a 15 MHz Arbitrary Waveform Generator (HP 33120A), and the output was amplified by a Hafler (P1500) Professional Amplifier and bandpassed at 8-16 KHz by a Stewart VBF8 Filter. Noise levels were measured with a sound level meter (RS 33-2055) in seven distinct locations within the chamber and ranged within 3 dB of the selected intensity. Immediately following the 1 hr exposure, animals were cardially perfused with 4% paraformaldehyde and the brain was quickly dissected and processed as described above.

Detection and Quantification of cFos positive cells. Adult *Vglut3*$^{+/+}$ and *Vglut3*$^{-/-}$ brains exposed to noise (80 dB or 120dB) and no noise were collectively processed for neuronal activity using immunoreactivity against the immediate early gene, cFos. Brainstem tissue sections were postfixed in 2% paraformaldehyde for 10 minutes, permeablized in 0.1% PBST, and endogenous peroxidase quenched using 1% H_2O_2, 10% Methanol in 1X PBS for 30 min. Tissue was blocked for 1 hr in 5% BSA and 1% Serum in 1XPBS followed by overnight incubation with primary antibody at 4˚C (cFos 1:8000 F7799, Sigma). The folliowing day tissue was incubated for 1 hour in block solution containing HRP conjugated secondary antibody (1:100, donkey anti-rabbit, Jackson Immunoresearch). Signal detection was accomplished by incubating tissue in DAB for at least 7 min. Nuclei were visualized using a DAPI fluorescent counterstain (1:1000, Life Technologies). Immunohistological staining was repeated multiple times with no limitations in repeatability observed.

10X images of right and left cochlear nuclei containing the major subdivisions—dorsal cochlear nucleus (DCN), ventral cochlear nucleus (VCN) and granule cell area (Gr)—were acquired. Images were collected by ENF from every other cross section to eliminate double counting a positive cell during quantification. To ensure blind analysis, all images were then randomized by other lab members (who are not authors) using list-randomizing software, and returned to ENF for quantification. The randomized code was revealed to ENF following blind quantification of all images. Using *ImageJ* the cochlear nuclei and major subdivisions were outlined and measured to generate the area. Major CN subdivisions were determined by comparing DAPI stained images to Nissl stained images of mouse CN [S10]. Positive cFos cells were quantified as described [S11] and neuronal densities were calculated for the total CN area, as well as for DCN, VCN and Gr areas.

Statistical Analyses. Total counts were sent to the Biostatistics Core Facility for analyses prior to revealing genotypes and hypotheses. SAS (version 9.4, SAS Institute Inc., Cary, NC, USA) software was used to construct a linear mixed model for total CN neuronal density with fixed genotype, exposure, and genotype-exposure interaction effects. A random animal effect was included in order to account for the within animal correlation due to measuring neuronal density on both the right and left sides of animals. Residual diagnostics were conducted to check model assumptions, and the analyses were repeated for each of the CN areas.

Test for normality was performed and the use of parametric testing-correct. Normality was tested within the genotype-exposure subgroups, and in general, producing no significant evidence (at the 5% level) against the assumption of normality according to the Shapiro-Wilk test for normality. Residual diagnostics also did not suggest alarming violations of the normality assumption. Since inherent dependence within animals was present, as each animal has more than one measurement (right and left sides), the assumption of independence is violated. We accounted for this by incorporating the random animal effect in the linear mixed model. The estimate of variance within each group was analyzed using a Least Squares Means output, which revealed standard error estimates for mean response in each group. Our values indicated similar variance between groups with standard error ranging from 4.3 to 5.6.

Auditory Brainstem Responses (ABR). P60 and P240 CD1 mice of either sex were anesthetized (100mg/kg ketamine, 12 mg/kg xylazine, i.p.) and fitted with needle electrodes inserted subcutaneously behind the ear (active), at the vertex (reference), and in the back (ground). ABR potentials were evoked with 8-ms tone pips (1-ms rise—fall). The response was amplified (10,000X), filtered with a custom filter (300 Hz – 3kHz) and averaged in TestPoint data acquisition system. Sound levels were raised in 5 dB SPL steps up to 90 dB SPL SPL. At each sound level, 1000 responses were averaged, with an artifact reject feature. ABR threshold was

defined as the lowest sound level where response peaks were clearly present, read by eye from stacked waveforms obtained at 5 dB SPL sound pressure intervals (up to 90 dB SPL SPL). Thresholds corresponded to a level where the peak-to-peak response amplitude began to rise.

Vestibular function. Semicircular canal and vestibule function was assessed in P60 and P240 CD1 mice of either sex using the spin test. Mice were subjected to horizontal rotations (250 r.p.m) on a rotating platform for 20 seconds. Immediately following, the number of nystagmus eye movements were observed under a dissection microscope at 4X and recorded for 45 seconds. The number of nystagmus recorded in the first 10 seconds following rotation was averaged and compared between young and aged CD1 mice. Statistical differences were measured using an unpaired student's t-test (GraphPad Prism).

Detailed Author Contributions

ENF performed most experiments and analyses and contributed portions of the text and figures. AD performed the immunohistochemistry with nociceptive markers that initiated this study. TM, GC and FM performed the noise avoidance experiments. AKH quantified the cFos levels in vestibular and trigeminal nuclei. RS and RE provided the *Vglut3* KO mice. MCL was involved in the genesis of the project, provided expert advice throughout, particularly in the design of noise avoidance assay, and evaluated the cochleae after noxious and innocuous noise exposure. JG-A supervised all aspects of the project, performed some of the initial immunohistochemistry, formulated the hypotheses, chose the animal models, developed the noise avoidance and noxious noise assays, and wrote the manuscript.

Supplemental References

S1. Seal, R.P., Akil, O., Yi, E., Weber, C.M., Grant, L., Yoo, J., Clause, A., Kandler, K., Noebels, J.L., Glowatzki, E., et al. (2008). Sensorineural deafness and seizures in mice lacking vesicular glutamate transporter 3. Neuron *57*, 263-275.

S2. Kiang, N. (1984). Peripheral neural processing of auditory information. In The Nervous System. Sensory Processes Part 1, J.M. Brookhart and V.B. Mountcastle, eds. (Bethesda MD: American Physiological Society).

S3. Berglund, A.M., and Ryugo, D.K. (1986). A monoclonal antibody labels type II neurons of the spiral ganglion. Brain research *383*, 327-332.

S4. Hafidi, A. (1998). Peripherin-like immunoreactivity in type II spiral ganglion cell body and projections. Brain research *805*, 181-190.

S5. Garcia-Anoveros, J., Samad, T.A., Zuvela-Jelaska, L., Woolf, C.J., and Corey, D.P. (2001). Transport and localization of the DEG/ENaC ion channel BNaC1alpha to peripheral mechanosensory terminals of dorsal root ganglia neurons. The Journal of neuroscience : the official journal of the Society for Neuroscience *21*, 2678-2686.

S6. Balaban, C.D., Zhou, J., and Li, H.S. (2003). Type 1 vanilloid receptor expression by mammalian inner ear ganglion cells. Hearing research *175*, 165-170.

S7. Caterina, M.J., Leffler, A., Malmberg, A.B., Martin, W.J., Trafton, J., Petersen-Zeitz, K.R., Koltzenburg, M., Basbaum, A.I., and Julius, D. (2000). Impaired nociception and pain sensation in mice lacking the capsaicin receptor. Science *288*, 306-313.

S8. Castiglioni, A.J., Remis, N.N., Flores, E.N., and Garcia-Anoveros, J. (2011). Expression and vesicular localization of mouse Trpml3 in stria vascularis, hair cells, and vomeronasal and olfactory receptor neurons. The Journal of comparative neurology *519*, 1095-1114.

S9. Wang, Y., Hirose, K., and Liberman, M.C. (2002). Dynamics of noise-induced cellular injury and repair in the mouse cochlea. Journal of the Association for Research in Otolaryngology : JARO *3*, 248-268.

S10. Berglund, A.M., and Brown, M.C. (1994). Central trajectories of type II spiral ganglion cells from various cochlear regions in mice. Hearing research *75*, 121-130.

S11. Brown, M.C., and Liu, T.S. (1995). Fos-like immunoreactivity in central auditory neurons of the mouse. The Journal of comparative neurology *357*, 85-97.